Advances in Manufacturing (manuscript as accepted)
September 2018, Volume 6, Issue 3, pp 345–353
DOI: https://doi.org/10.1007/s40436-018-0229-6

The stability of turning processes in case of periodic chip formation

Gergely Gyebrószki · Daniel Bachrathy · Gábor Csernák · Gabor Stepan

Received: 10 November 2017 / Accepted: 03 July 2018

Abstract The prediction of chatter vibration is influenced by many known complex phenomena, still the predictions can be uncertain. We present a new effect which can significantly change the stability properties of cutting processes. It is shown that the microscopic environment of the chip formation can have large effect on the macroscopic properties. In this work, a combined model of the surface regeneration effect and the chip formation is used to predict the stability in turning processes. In the chip segmentation sub-model, the primary shear zone is described with the corresponding material model along layers together with the thermodynamical behaviour. The surface regeneration is modelled by the time-delayed differential equation. Numerical simulations show, that the time scale of chip segmentation model is significantly smaller than the time scale of the turning process, therefore, averaging methods can be used. Due to the non-linear effects, the chip segmentation can decrease the average shear force leading to decreased cutting coefficients. The proper linearization of the equation of motion leads to an improved description of the cutting coefficients. It is shown that the chip segmentation may significantly increase the stable domains in the stability charts, furthermore, with selecting proper parameters, unbounded stability domains could be reached.

Keywords chip formation · chatter · turning · delay

The research leading to these results has received funding from the European Research Council under the European Union's Seventh Framework Programme (FP7/2007-2013) ERC Advanced grant agreement №340889.

Gergely Gyebrószki, Daniel Bachrathy, Gabor Stepan
Department of Applied Mechanics,
Budapest University of Technology and Economics, Budapest, Hungary
Tel.: +31-1-463-1111
E-mail: gyebro@mm.bme.hu, bachrathy@mm.bme.hu, stepan@mm.bme.hu

Gábor Csernák
MTA-BME Research Group on Dynamics of Machines and Vehicles, Budapest, Hungary E-mail: csernak@mm.bme.hu

Nomenclature

Symbol	Definition [unit]
a	Constant in the constitutive equation [−]
b	Constant in the constitutive equation [−]
C	Constant in the constitutive equation [−]
c	Heat capacity $\left[\mathrm{J\,kg^{-1}\,K^{-1}}\right]$
E	Modulus of elasticity [MPa]
h_0	Initial chip thickness [m]
K	Time scale of chip formation [s]
L	Acting length of normal stress [m]
r	Energy ratio [−]
T_i	Temperature of the shear zone band i [K]
T_w	Temperature of the workpiece [K]
$\tilde{t}$	Dimensionless time of chip formation [−]
$\hat{t}$	Dimensionless time of turning [−]
v	Cutting speed [m/s]
δ	Thickness of deformation layer [m]
γ_i	Shear strain in shear zone band i [−]
Φ	Angle of the shear plane [rad]
Ω	Angular velocity of workpiece [rad/s]
ω_n	Natural frequency of machine-tool system [rad/s]
ρ	Density $\left[\mathrm{kg\,m^{-3}}\right]$
κ	Relative damping [−]
τ_Φ	Shear stress in case of continuous chip formation $\left[\mathrm{N\,m^{-2}}\right]$
ξ	Dimensionless parameter of chip formation [−]
η	Dimensionless parameter of chip formation [−]
ζ	Dimensionless parameter of chip formation [−]

1 Introduction

The proper mathematical description of harmful chatter vibrations in cutting processes is still challenging and the corresponding stability charts can be unreliable even after half-century-long research [2–6]. Although the surface regeneration effect (which is the main source of these self-excited vibrations) can be modelled properly by means of delayed differential equations [1], undesired vibrations are also influenced by many different phenomena. Some of them are the dynamical uncertainty [16], non-linear cutting force characteristic [19], process damping phenomena (explained by the flank face contact [17, 18]), velocity dependent chip thickness [14, 20, 24], influence of material microstructure [25] or short-delay effect [1], nose radius effect [21], fly-over effect [22], etc.

In this work we try to highlight, that the fluctuation of the shear stress in the primary shear zone can lead to significantly different stability properties during turning.

The surface regeneration is described by the traditional delay differential equation (DDE) based on the cutting force characteristic, the dynamic properties of the machine-tool/milling-tool/workpiece system and the cutter engagement conditions (chip thickness and chip width).

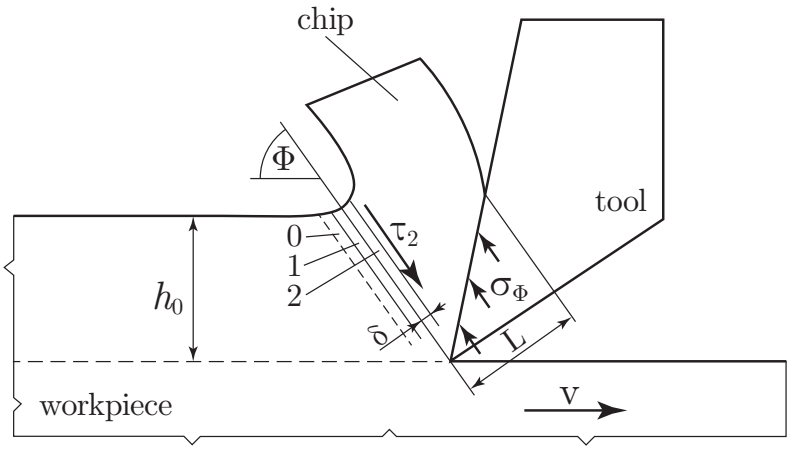

Fig. 1 Model of shear zone in case of milling. Numbers indicate shear layers.

The mathematical modelling of chip formation and segmentation is undoubtedly a difficult task. Even simple models could lead to complex non-linear and time-delayed differential equations. Furthermore, if thermodynamical behaviour is also taken into account, the resulting model is usually high dimensional.

In recent works of Csernák and Pálmai [8–10], a 4-dimensional non-linear system of differential equations is elaborated to model chip segmentation, which exhibits periodic, aperiodic and chaotic behaviour, and can be considered as one of the simplest system of differential equations describing thermomechanical effects in a satisfactory manner.

We present a coupled system of the well-known delay-differential equation of turning [1] and the 4-dimensional model of chip segmentation and examine the stability properties of the resulting model. Our primary goal is to show the qualitative behaviour of the interconnected system.

This paper first focuses on a mathematical model which includes the complex thermomechanical behaviour of the shear zone. Afterwards we briefly introduce the delay-differential equation (DDE) of orthogonal turning, which is related to the phenomenon of *regenerative machine tool chatter* [2]. Then, the coupled model of turning and chip formation is presented. The multi-scale nature of the coupled system is shown and a simple averaging is used to replace the dynamics of the chip formation. It is shown, that in case of periodic chip formation, the average value of shear stress may be lower than in case of continuous chip formation, thus this effect can shift the stability boundaries.

2 Model of chip formation

The description of the cutting force as a function of the chip thickness is an important part of the modelling. The 4D model of chip segmentation presented in [10] is used to examine the shear process in two deformation bands (1 and 2) of thickness δ. (See Fig. 1.) In layer 0, no deformation occurs, however, heat may flow from layer 1 to layer 0. Two equations of the system correspond to the

mechanical balance of the shear stresses and the corresponding component of the normal stress acting on the tool (σ_Φ, L, see Fig. 1.), while the other three energy equations describe the thermal dynamics of the layers. Here only the final system of differential equations is presented for the dimensionless shear stresses τ_i and shear layer temperatures T_i. For the detailed derivation see [10]. Note that the dimensionless shear stress in layer 1 is the ratio between the current shear stress and the shear stress τ_Φ in case of continuous chip formation.

$$\dot{\tau}_2(\tilde{t}) = (1 - F_1(\tau_1, T_1) - F_2(\tau_2, T_2)), \tag{1}$$

$$\tau_1(\tilde{t}) = p\,\tau_2(\tilde{t}) + s, \tag{2}$$

$$\dot{T}_0(\tilde{t}) = \zeta(T_1(\tilde{t}) - 2\,T_0(\tilde{t})) - \xi\,T_0(\tilde{t}), \tag{3}$$

$$\dot{T}_1(\tilde{t}) = \eta\,\tau_1(\tilde{t})F_1(\tau_1, T_1) - \zeta(2\,T_1(\tilde{t}) - T_2(\tilde{t}) - T_0(\tilde{t})) - \xi(T_1(\tilde{t}) - T_0(\tilde{t})), \tag{4}$$

$$\dot{T}_2(\tilde{t}) = \eta\,\tau_2(\tilde{t})F_2(\tau_2, T_2) - (\xi + \zeta)(T_2(\tilde{t}) - T_1(\tilde{t})). \tag{5}$$

Here $\tilde{t} = t/K$ is the dimensionless time, where K is the time scale and ξ, ζ and η are compound dimensionless system parameters. p is a technological system parameter – typically its value is close to 1 – and $s = 1 - p$ is an integration constant in Eq. (2) connecting the shear stress of layers 1 and 2 [8]. F_i is the velocity of shear strain ($\dot{\gamma}_i(t)/\dot{\varepsilon}_\Phi$) in layer i. These are summarized below:

$$F_i(\tau_i, T_i) = \frac{T_i + 1}{C + 1} \exp\left(\frac{\tau_i - 1 + a(T_i - C)}{b(T_i + 1)}\right), \tag{6}$$

$$K = \frac{\tau_\Phi\,h(\tilde{t})^2}{E\,L\,v\,\sin^2(\Phi)\,\cos(\Phi)}, \tag{7}$$

$$\xi = \frac{K\,v\,sin(\Phi)}{\delta}, \tag{8}$$

$$\eta = \frac{K\,v\,r\,\tau_\Phi\,cos(\Phi)}{c\,\rho\,\delta\,T_w}, \tag{9}$$

$$\zeta = \frac{4\,K\,\lambda}{c\,\rho\,\delta^2}. \tag{10}$$

The time scale depends on the chip thickness h, the modulus of elasticity E, and the angle of the shear plane Φ, while the compound system parameters mainly depend on thermal parameters: heat capacity c, density ρ, thermal conductivity λ, temperature of the workpiece T_w, and energy ratio $r \approx 0.95$ corresponding to a nearly adiabatic process. The parameters a, b are constant values characterising the material and $C = T_\Phi$ is the temperature of the shear zone in case of continuous chip formation and v is the cutting velocity.

In this model, the angle Φ of the shear plane, the contact length L of the chip and tool and the chip thickness $h(\tilde{t}) = h_0$ are considered to be constant [8].

It has been shown [9, 10], that the 4D model of chip formation can exhibit periodic and even chaotic behaviour. Hopf–, Fold and period-doubling bifurcations with respect to the system parameter ξ are shown in Fig. 2.

The bifurcation chart shows, that continuous chip formation can lose its stability, which leads to a fluctuation in the shear force (see the time domain simulation in Fig. 3). In practice, the saturation of the shear force close to zero value describes the saw-tooth-like chip segmentation (as represented in our high speed camera measurements in Fig 4). The chaotic behaviour predicted by the model has already been presented in [15].

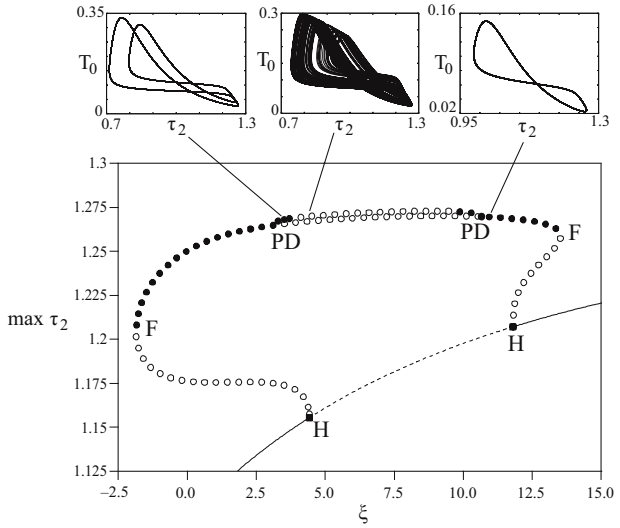

Fig. 2 Bifurcations of chip formation model with respect to system parameter ξ, published in [10]. Letters indicate, H: Hopf, F: Fold bifurcations and PD: Period doubling.

Parameter	Value [unit]
k	0.008 [−]
T_w	300 [K]
E	200×10^{-9} [Pa]
r	0.95 [−]
a	0.3 [−]
b	0.012 [−]
C	1 [−]
Φ	0.572 [rad]
δ	1.25×10^{-5} [m]
λ	16 [N/(msK)]
$c\,\rho$	500×7900 $\left[\mathrm{JK^{-1}m^{-3}}\right]$
R	0.03 [m]
κ	0.05 [−]
ω_n	3100 [rad/s]
L	7.5×10^{-4} [m]
h_0	1×10^{-3} [m]
Ω	500 $[rad/s]$
p	1.012 [−]
s	-0.012 [−]

Table 1 Parameter values in case of a realistic machining operation of steel workpiece. Material parameters are corresponding to austenitic (stainless) steel [9, 10].

3 Delay-differential equation of orthogonal turning

In this section, the traditional linear orthogonal turning model with surface regeneration effect is presented (see Fig. 5) [1, 3, 23]. As in most of the cases there is a single dominant mode of the system, it is suitable to use a single degree of freedom mass-spring-damper model [1, 2, 11]. The governing equation of the system is given by:

$$m\,\ddot{x}(t) + c\,\dot{x}(t) + k\,x(t) = k_1\,w(h_0 - x(t) + x(t - \tau_r)), \tag{11}$$

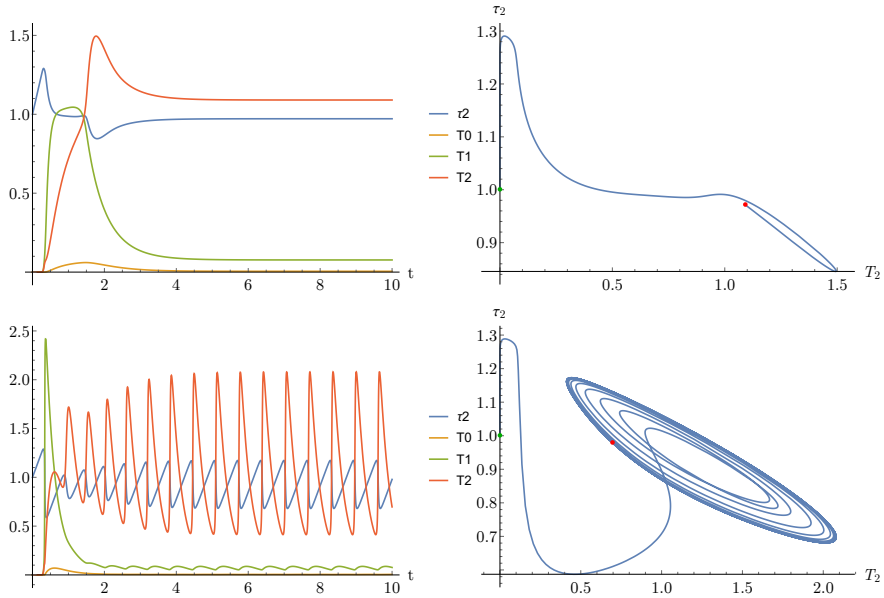

Fig. 3 Time domain simulation of Eq. (1). Above: fixed point solution $h_0 = 0.001$, Below: periodic orbit solution $h_0 = 0.0018$ - saw-tooth-like shear stress indicates similarly shaped chip. All other parameters are listed in Table 2. Shear stress and layer temperature values are dimensionless.

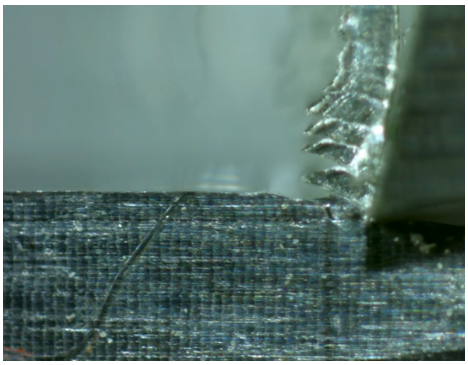

Fig. 4 High-speed camera picture of chip saw-tooth-like chip segmentation in case of milling.

where the parameters are: mass m, damping c, stiffness k, cutting coefficient k_1, chip width w, feed per revolution h_0, time delay $\tau = 2\pi/\Omega$ and spindle speed Ω. The right hand side of Eq. (11) expresses that the force acting on the tool is proportional to the actual chip thickness $h(t) = h_0 - x(t) + x(t - \tau_r)$, which is governed by the current tool position and the position in the previous revolution.

The number of parameters can be reduced by using their dimensionless variants respectively (dimensionless time $\hat{t} = t\,\omega_n$ with natural angular frequency $\omega_n = \sqrt{k/m}$, damping ratio $\kappa = c/2\sqrt{m/,k}$, dimensionless chip width $H_w = w\,k_1/k$, dimensionless time delay $\hat{\tau} = 2\pi\omega_n/\Omega$, dimensionless spindle speed $\hat{\Omega} = \Omega/\omega_n$).

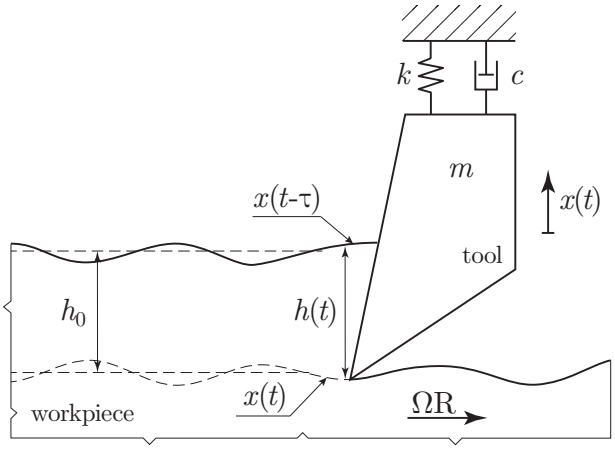

Fig. 5 Simple mechanical model of orthogonal turning with surface regeneration effect.

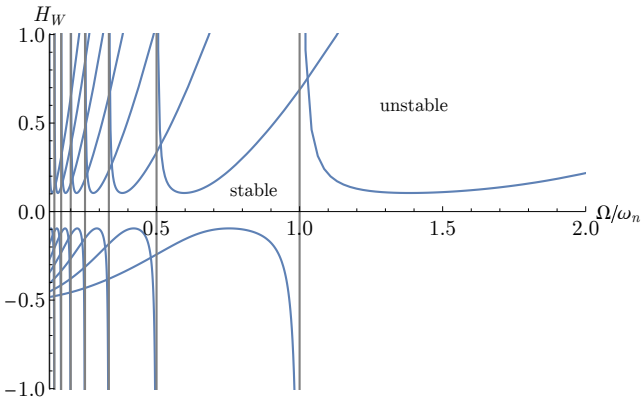

Fig. 6 Stability chart of the DDE of turning, with respect to Ω and H_w parameters.

Rearranging Eq. (11), the time-delayed governing equation is written as follows [1]:

$$\ddot{x}(\hat{t}) + 2\,\kappa\,\dot{x}(\hat{t}) + x(\hat{t}) = H_w\,h(\hat{t}), \tag{12}$$

$$h(\hat{t}) = h_0 - x(\hat{t}) + x(\hat{t} - \hat{\tau}). \tag{13}$$

The stability boundaries of Eq. (12) are known analytically [1], and can be shown as the region below the so-called stability lobe structures in the stability chart (see Fig. 6).

In the subsequent section, the two above presented models are combined. The cutting coefficient in the turning model is determined based on the shear force in the chip formation model Eq. (1), while the chip thickness in the chip formation model is considered as a time dependent variable of the turning model Eq. (13).

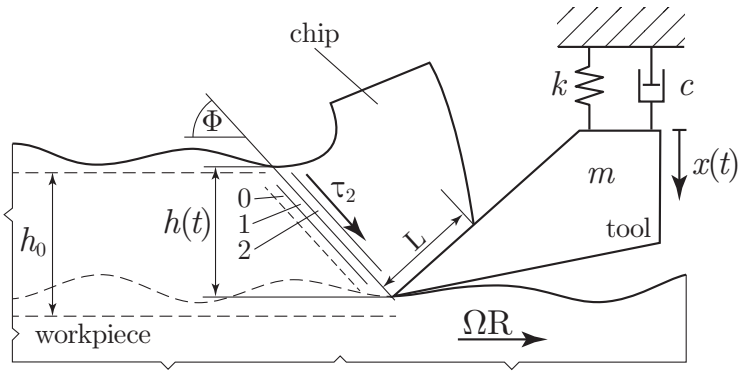

Fig. 7 Model of shear zone in case of orthogonal turning with surface regeneration effect. Numbers indicate shear layers.

4 Coupled system of turning and chip formation

Recall that the dimensionless time of the delay differential equation of the turning is $\hat{t} = \omega_n\, t$, but the 4D model of chip segmentation has a different time scale $\tilde{t} = t/K$ (see Eq. (7)). We transform the corresponding equations to match the dimensionless time of turning; substituting $\tilde{t} = \hat{t}/(K\,\omega_n)$ yields:

$$
\begin{aligned}
\dot{\tau}_2(\hat{t}) &= (1 - F_1 - F_2)/(K\,\omega_n), \\
\tau_1(\hat{t}) &= p\,\tau_2(\hat{t}) + s, \\
\dot{T}_0(\hat{t}) &= (\zeta(T_1(\hat{t}) - 2\,T_0(\hat{t})) - \xi\,T_0(\hat{t}))/(K\,\omega_n), \\
\dot{T}_1(\hat{t}) &= (\eta\,\tau_1(\hat{t})F_1 - \zeta(2\,T_1(\hat{t}) - T_2(\hat{t}) - T_0(\hat{t})) - \xi(T_1(\hat{t}) - T_0(\hat{t})))/(K\,\omega_n), \\
\dot{T}_2(\hat{t}) &= (\eta\,\tau_2(\hat{t})F_2 - (\xi + \zeta)(T_2(\hat{t}) - T_1(\hat{t})))/(K\,\omega_n),
\end{aligned}
\tag{14}
$$

where the cutting speed is $v_c = \Omega\, R$.

The two subsystems are fully coupled. The chip formation is influenced by the chip thickness $h(\hat{t})$ through the parameter K (see Eq. (7) as a parametric excitation. In our model we assume, that the cutting force is equivalent to the resultant of the shear stress τ_2 at the area of the principal shear plane $w\,h(\hat{t})/\sin(\Phi)$ (see Fig. 8).

As the actual chip thickness is $h(\hat{t}) = h_0 - x(\hat{t}) + x(\hat{t} - \tau)$, and the force acting on the tool is $\tau_2\,\tau_\Phi\,w\,h(\hat{t})/\sin(\Phi)$, the x-directional component of the force is $\tau_2\,\tau_\Phi\,w\,h(\hat{t})$. This couples the chip formation to the DDE of turning in the backwards direction and therefore the right hand side of Eq. (12) changes to:

$$
\ddot{x}(\hat{t}) + 2\,\kappa\,\dot{x}(\hat{t}) + x(\hat{t}) = \frac{w}{k}\,\tau_2(\hat{t})\,\tau_\Phi\,h(\hat{t}). \tag{15}
$$

Note, that in our model, if we consider continuous chip formation with constant shear stress ($\tau_2\,\tau_\Phi$) then the cutting coefficient is $k_1 = \tau_2\,\tau_\Phi$ in Eq. (11).
Introducing the dimensionless displacement $\hat{x} = x/h_0$ and chip thickness $\hat{h}(\hat{t}) = h(\hat{t})\frac{w\,\tau_\Phi}{h_0\,k}$, Eq. (15) can be written as:

$$
\ddot{\hat{x}}(\hat{t}) + 2\,\kappa\,\dot{\hat{x}}(\hat{t}) + \hat{x}(\hat{t}) = \tau_2(\hat{t})\,\hat{h}(\hat{t}). \tag{16}
$$

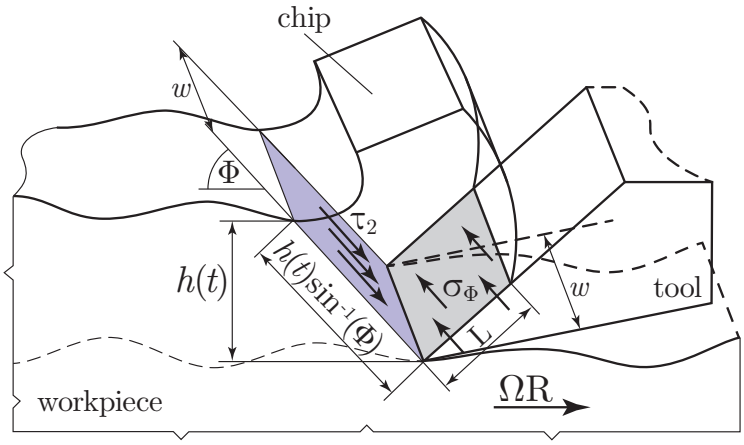

Fig. 8 The shear plane ■ and the area of chip-tool contact ■. The mechanical balance of τ_2 times the area of shear plane ($w\,h(t)/\sin(\Phi)$) and the corresponding component of the stress acting on the chip (σ_Φ) times the area of contact ($w\,L$) can be seen.

Note that by abuse of notations, the hat symbols ($\hat{\square}$) are discarded in the following sections.

The results of numerical simulations for the combined model are shown in Fig. 9. In the first case, the simulation shows continuous chip formation with almost constant shear force (yellow ■ line) together with the transient oscillation of the tool (blue ■ line). In the second case, the stability loss is only visible in the chip formation level, leading to large oscillation in the shear force at very high frequency, while the tool motion still shows a relatively slow transient oscillation.

Mathematically, this solution is unstable, however, from the practical point of view the tool vibration tends to very small amplitude oscillation creating negligible surface error and insignificant extra load on the cutting edge. It is clear that the tool motion with the relatively large time constant can not react to the very high frequency shear oscillation. Based on averaging in multi-scale methods [27], its average value is sufficient to be used during the simulation. The details of the averaging method are described next.

5 Averaging of the fast dynamics of chip formation

In the simplest form of the method of multiple scales, the variation of the chip thickness in Eq. (15) is considered to be quasi-static. During the simulations, first, the stationary solution of the shear plane must be determined as a function of the chip thickness, then its average can be used in Eq. (15) as $\tau_2(h(t))$.

If we consider the strong non-linearities in the chip formation model, then the bifurcations along the chip thickness parameter h_0 must be described too.

By carrying out numerical simulations with realistic parameters, we obtained the following bifurcation diagrams. In Fig. 10, simulation results after sufficiently long numerical integration are shown, with the maximum, minimum and average of τ_2 values with respect to h_0.

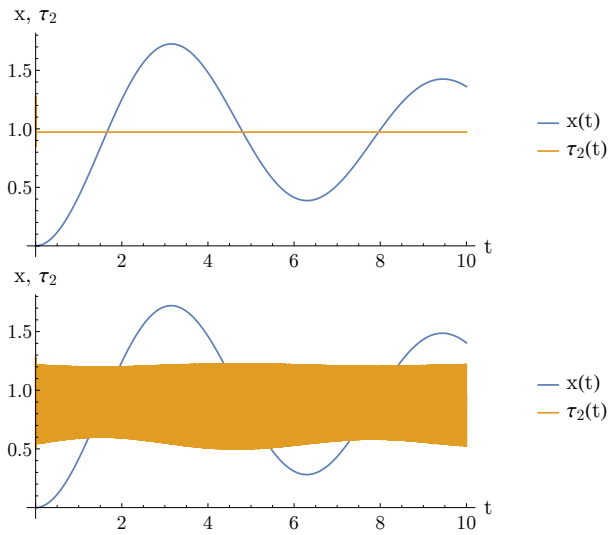

Fig. 9 Top to bottom: $h_0 = 1.4\times10^{-3}, 1.7\times10^{-3}$[m], continuous and periodic chip formation. The oscillation of τ_2 is much faster due to the significant difference in the time scale of turning and chip formation. The shear stress τ_2 values are dimensionless, the units of displacement x is [m/100].

It can be seen, that there is a critical chip thickness ($h_{0,\text{crit}}$), which separates the fixed point solutions from the periodic solutions. In case of periodic chip formation, the average value of τ_2 is decreasing as the chip thickness increases due to the non-linearities. Note, that the stability charts are usually plotted as a function of cutting speed $v = \Omega R$ and chip width H_w (see Fig 6.), so the influence of Ω is also examined. It is important to note that the critical chip thickness is not very sensitive to the cutting speed. In the example, these values were $h_{0,\text{crit}} = 1.69\times10^{-3}$[m] and $h_{0,\text{crit}} = 1.75\times10^{-3}$[m] for cutting speeds $v = 6$[m/s] and $v = 30$[m/s] respectively. Although these critical chip thickness values are unusually large, at the level of mathematical modelling these can be altered easily. In case of measurements one may found suitable material and cutting conditions to achieve considerably lower critical chip thicknesses.

We must note that as the shear stress reaches zero ($\tau_2 = 0$), the chip formation model loses its validity, because it does not deal with non-smooth case of discontinuous chip formation.

We can see in Fig. 10 that the average shear stress can be approximated as:

$$\tau_2(h) = \begin{cases} \overline{\tau}_2 & h_0 \leq h_{crit} \\ \alpha\, h_0^{\beta} + \gamma & h_0 > h_{crit} \end{cases} \tag{17}$$

where α, β and γ are coefficients fitted to the simulated average of $\tau_2(h)$. Based on numerical simulations for larger h_0 parameters and based on Fig. 10, we used the approximation $\gamma = 0.4$. The graph of the fitted functions in Fig. 11 has a very good correlation to the average shear stress values. The variation of the coefficients are plotted in Fig 12 with respect to the spindle speed. It is visible, that the cutting speed has negligible effect on the parameters. After the starting

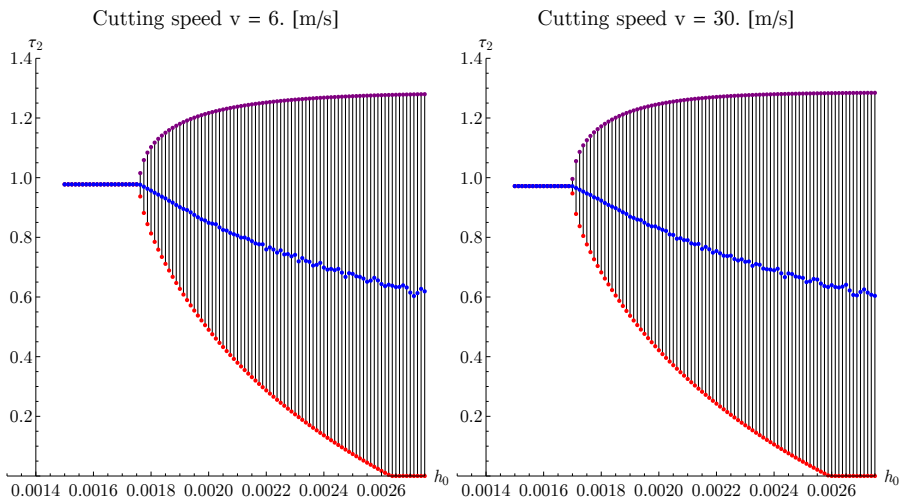

Fig. 10 Minimum, maximum and average values of τ_2 in case of varying h_0 and v. Legend: Blue ■ indicates average, red ■ indicates minimum, purple ■ indicates maximum value of τ_2 in case of fixed point or periodic solution.

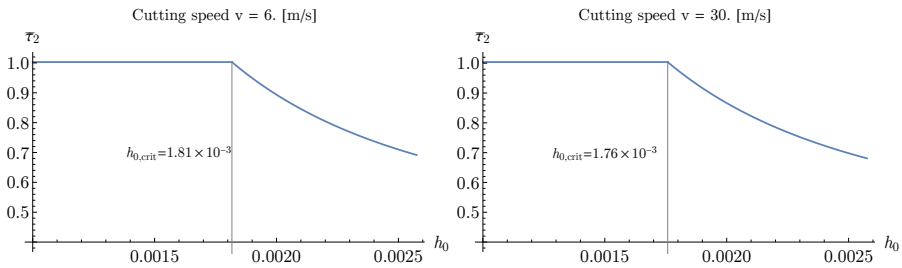

Fig. 11 Power function fitted on the average values of $\tau_2(h_0)$. Left: $v = 6[\mathrm{m/s}], \alpha = 1.164 \times 10^{-6}, \beta = -2.085, \gamma = 0.4, R^2 = 0.0013$. Right: $v = 30[\mathrm{m/s}], \alpha = 1.81 \times 10^{-6}, \beta = -2.005, \gamma = 0.4, R^2 = 0.0014$. Here the shear stress values are dimensionless.

point of the segmentation at bifurcation parameter $h = h_{0,crit}$, the shear force tends to a decreased value with approximate decay rate of 0.7.

The function Eq. (17) can be substituted formally to Eq. (15):

$$\ddot{x}(t) + 2\,\kappa\,\dot{x}(t) + x(t) = \tau_2(h(t))\,h(t). \tag{18}$$

For the linear stability computation, first, the Taylor expansion of the right-hand-side according to the state variables $x(t)$ and $x(t-\tau)$ must be derived:

$$\begin{aligned} w\,\tau_2(h(\hat{t}))\,h(\hat{t}) &= w\,\tau_2(h_0 - x(\hat{t}) + x(\hat{t}-\tau))\,(h_0 - x(\hat{t}) + x(\hat{t}-\tau)) \approxeq \\ & w\,\tau_2(h_0)\,h_0 + w\left(\tau_2(h_0) + \frac{\partial \tau_2}{\partial h_0} h_0\right)(-x(\hat{t}) + x(\hat{t}-\tau)) + \text{h.o.t.} \end{aligned} \tag{19}$$

In the linear stability analysis, the higher order terms and the static components can be eliminated (see [1]). The characteristic equation of the delay differential equation of turning in case of averaged τ_2 can be written as:

$$(i\,\omega)^2 + 2\,\kappa\,(i\,\omega) + 1 = H_w\,(\tau_2(h_0) + h_0\,\tau_2'(h_0))\,(-1 + e^{-(i\,\omega)\,\tau}). \tag{20}$$

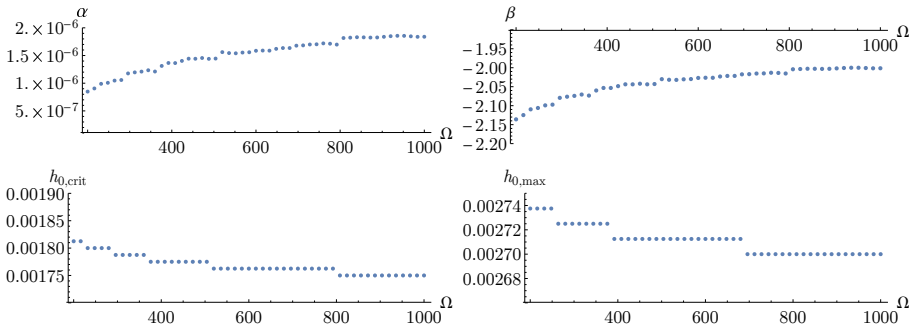

Fig. 12 The parameters of fitted functions and critical chip thickness / maximal chip thickness values [m] with respect to Ω [rad].

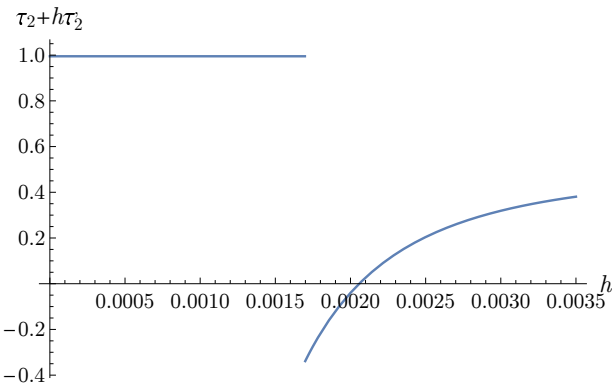

Fig. 13 Plot of $\tau_2 + h\,\tau_2'$ as appears in the characteristic polynomial.

In the range where $\tau_2(h_0)$ is almost constant, the coefficient of the linear part would be $w\,\tau_2(h_0)$, which leads to the traditional turning model (see Section 2). However, in the segmentation range, the derivative term of $\partial\tau_2/\partial h_0$ can radically decrease value of the already decreased value of average shear stress in the coefficient, furthermore, it can shift it to a negative value, too (see. Fig 13).

The stability regions for Eq. (20) based on the D-subdivision method [1] were constructed using Multi-Dimensional Bisection Method [12]. For a fixed cutting speed, the stability boundary is plotted along the nominal chip thickness h_0 for cases considering or neglecting the derivative $\tau_2'(h)$ of the average (see Fig. 14).

The results show, that taking the proper derivative of the average shear force into account, the stable region further increases. The connection between the sudden change in the stability limit and the coefficient on the right-hand-side can be clearly identified by comparing Fig. 13 and Fig 10. In the case at the critical value of h_0^* where the coefficients crosses the zeros line, theoretically, all the depth of cut at any spindle speed would be stable.

We also present the stability charts as a function of the spindle speed and the cutting depth for different chip width values, to show the vertical shift in the lobe structure. Fig. 15 shows the increasing stable domain in the range $h_0 \in 0 \ldots h_0^*$, while Fig. 16 presents the decreasing stable domain in $h_0 \in h_0^* \ldots 0.00275$ [m].

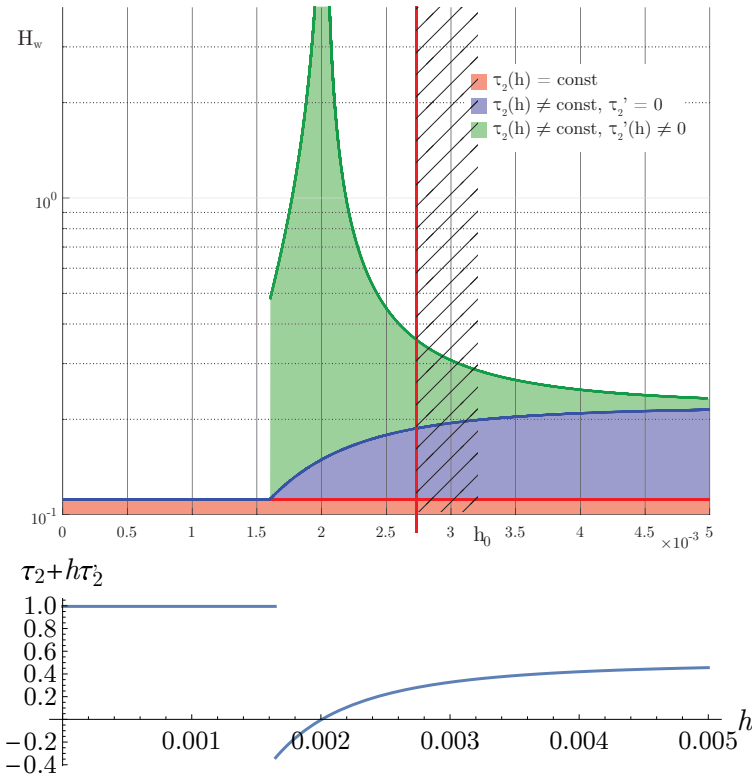

Fig. 14 Stability regions of the coupled system. Blue line indicates the case, where the derivative of the average with respect to h is neglected ($\tau_2(h) \equiv \overline{\tau}_2, \tau_2'(h) = 0$), green line indicates the case, when it is taken into account ($\tau_2'(h) \neq 0$).

Note, that this prediction is really sensitive to the fitted derivative of the average shear stress. We also found, that the $\tau_2 = \alpha\, h_0^{\beta}$ function can fit reasonably well at $\beta \approx -1$ value. However, in this case the terms $\tau_2(h_0)$ and $h_0\, \partial\tau_2/\partial h_0$ would cancel each other. This would predict that the cutting process is always stable in case of segmented chip for any parameters.

The selected form of the fitted parameters can lead to a different prediction, but all of them lead to the same conclusion, that the segmentation can radically improve the stability properties.

6 Conclusions

In this work, we combined the surface regeneration model of the turning process with the mathematical modelling of chip formation. It is shown that the time scale of chip formation is several magnitudes smaller than the time scale of turning, therefore the application of the simplest averaging method can be used to replace the dynamics of chip segmentation. Then the characteristic equation of the resulting system is analysed and its stability charts are presented.

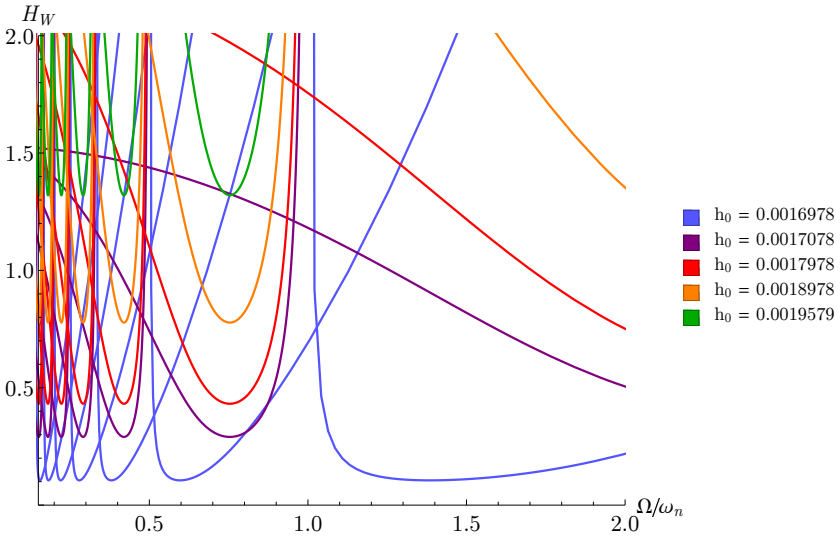

Fig. 15 Stability lobes in case of $h_{\text{crit}} < h < h^*$. See the increasing green domain in Fig. 14.

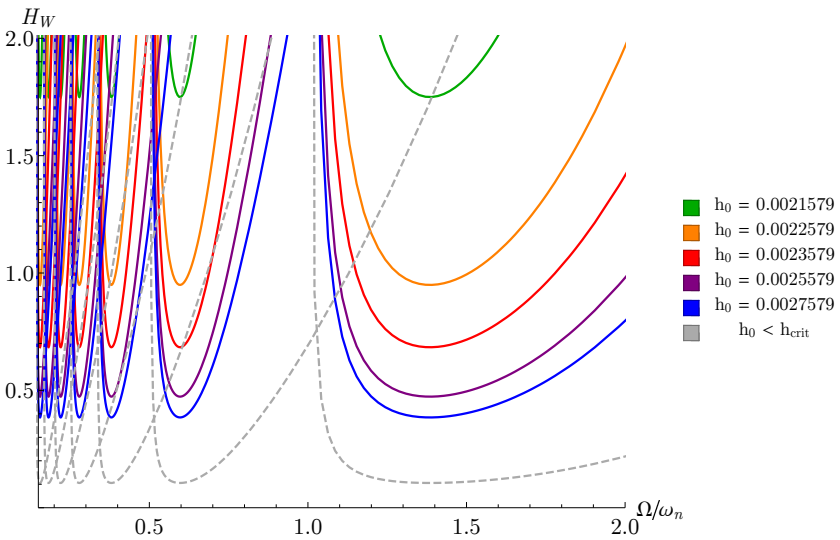

Fig. 16 Stability lobes in case of $h > h^*$. See the decreasing green domain in Fig. 14. which tends to the blue region – meaning an increase in the stable domain compared to the continuous chip formation.

We found, that increasing the chip thickness decreases the average shear stress in the shear layer if oscillatory chip formation (chip segmentation) begins, and thus it increases the stability, shifting the lobe structure upwards, see Fig. 14. This phenomenon could be utilized in case of flexible structures and hard-to-cut materials, where the chatter vibration is a great problem.

It is important to note that the chip formation model has a limited range of validity, once the shear stress in the shear layer reaches zero and the chip

breaks, the model is not applicable anymore (this is indicated by the vertical red border in Fig. 14). The chip formation model includes assumptions (for example the shear plane angle is considered constant) which makes experimental validation very complicated and valid only for that specific case, moreover these assumptions are usually not valid in the typical range of machining parameters in industrial applications.

The main goal of this work was to show the qualitative behaviour of the coupled model, that is, periodic chip formation can reduce the cutting force. This simplified model is a first step to show the importance of the critical range of chip formation and to highlight that modelling the shear layer could yield added value in the analytical process.

Acknowledgements The research leading to these results has received funding from the European Research Council under the European Union's Seventh Framework Programme (FP7/2007-2013) ERC Advanced grant agreement No. 340889 and it was supported by the Hungarian Scientific Research Fund – OTKA PD-112983 and the Janos Bolyai Research Scholarship of the Hungarian Academy of Sciences.

References

1. G. Stepan: Retarded dynamical systems: stability and characteristic functions *Longman Scientific & Technical, UK*, ISBN: 0-582-03932-0 (1989)
2. S. A. Tobias, W. Fishwick: Theory of regenerative machine tool chatter. *Engineer* **205**(199–203) 238–239 (1958)
3. S. A. Tobias: Machine Tool Vibration, *Blackie and Son Ltd.*, Glasgow, (1965)
4. Y. Altintas: Manufacturing Automation: Metal Cutting Mechanics. Machine Tool Vibrations, and CNC Design, *Cambridge university press* (2012)
5. J. Munoa, X. Beudaert, Z. Dombovari, Y. Altintas, E. Budak, C. Brecher, G. Stepan: Chatter suppression techniques in metal cutting, *CIRP Annals-Manufacturing Technology* 65 (2), 785-808
6. J. Tlusty, M. Polacek: The stability of the machine tool against self-exited vibration in machining. *Proceedings of the International Research in Production Engineering Conference*, ASME Press, Pittsburgh, 465–474 (1963)
7. J. Tlusty: Analysis of the state of research in cutting dynamics, *CIRP Annals* **27** 583–589 (1978)
8. Z. Pálmai, Chaotic phenomena induced by the fast plastic deformation of metals during cutting, *ASME Journal of Applied Mechanics* **73**: 240—245 (2006)
9. Z. Pálmai, G. Csernák: Chip formation as an oscillator during the turning process, *Journal of Sound and Vibration* **326**(3-5): 809–820 (2009)
10. G. Csernák, Z. Pálmai: Exploration of the chaotic phenomena induced by fast plastic deformation of metals, *The International Journal of Advanced Manufacturing Technology* **40**(3): 270–276 (2009)
11. Trent, E. M., Wright, P. K.: Metal Cutting, *Butterworth-Heinemann* **ISBN 978-0-750-67069-2** (2000)
12. D. Bachrathy, G. Stepan: Bisection method in higher dimensions and the efficiency number, *Periodica Polytechnica, Mechanical Engineering* **56**(2): 81–86. (2012)
13. H. T. Sykora, D. Bachrathy, G. Stepan: A theoretical investigation of the effect of the stochasticity in the material properties on the chatter detection during turning *Proceedings of the ASME 2017 Conference on Mechanical Vibration and Noise* August 6-9, (2017)
14. T. G. Molnár, T. Insperger, D. Bachrathy, G. Stepan: Extension of Process Damping to Milling with Low Radial Immersion, *International Journal of Advanced Manufacturing Technology* **89**:2545—2556. (2017)
15. R. S. Pawade, S. S.Joshi, Mechanism of Chip Formation in High-Speed Turning of Inconel 718, *Machining Science and Technology* **15**(1):132–152. (2011)
16. D. Hajdu, T. Insperger, G. Stepan: Robust stability analysis of machining operations, *International Journal of Advanced Manufacturing Technology* **88**(1):45–54 (2017)

17. Y. Altintas, M. Eynian, H. Onozuka: Identification of dynamic cutting force coefficients and chatter stability with process damping, *CIRP Ann Manuf Techn* 57(1):371–374 (2008)
18. E. Budak, L.T. Tunc: Identification and modeling of process damping in turning and milling using a new approach, *CIRP Ann - Manuf Techn* 59(1):403–408 (2010)
19. G. Stepan, Z. Dombovari, J. Munoa: Identification of cutting force characteristics based on chatter experiments, *CIRP Annals-Manufacturing Technology* **60**(1):113–116 (2011)
20. D. Bachrathy, G. Stepan: Bistable parameter region caused by velocity dependent chip thickness in milling process, *12th CIRP Conference on Modelling of Machining Operations. San Sebastian, Spain* **978-84-608-0866-4**:867–871 (2009)
21. E. Özlü, E. Budak, Analytical Modeling of Chatter Stability in Turning and Boring Operations—Part II: Experimental Verification, *Journal of Manufacturing Science and Engineering* **129** (2007)
22. Z. Dombovari, J. Munoa, R. Kuske, G. Stepan: Non-smooth torus to identify domain of attraction of stable milling processes *9th European Nonlinear Dynamics Conference (ENOC 2017), Budapest, Hungary* (2017)
23. M. Eynian, Y. Altintas: Chatter stability of general turning operations with process damping, *Journal of Manufacturing Science and Engineering* **131**(4):041005. (2009)
24. Budak E, Tunc LT (2010) Identification and modeling of process damping in turning and milling using a new approach. CIRP Ann - Manuf. Techn. 59(1):403–408
25. Cedergren, S., Frangoudis, C., Archenti, A. et al.: Influence of work material microstructure on vibrations when machining cast Ti-6Al-4V, *Int J Adv Manuf Technol* 84: 2277. (2016)
26. Bachrathy, D. (2015). Robust stability limit of delayed dynamical systems. Periodica Polytechnica. Engineering. Mechanical Engineering, 59(2), 74.
27. G. A. Pavliotis, A. M. Stuart: Multiscale Methods: Averaging and Homogenization, *Springer* **ISBN 978-0-387-73828-4** (2008)